Article ID: 1006-8775(2016) S1-0024-13

THE INFLUENCE OF PERSISTENT ANOMALY OF MJO ON ENSO

YAN Xin (严 欣)[1], JU Jian-hua (琚建华)[2], GAN Wei-wei (甘薇薇)[3]

(1. Resource Environment and Geosciences College, Yunnan University, Kunming 650000 China; 2. Yunnan Provincial Meteorological Bureau, Kunming 650000 China; 3. Sichuan Climate Center, Chengdu 610072 China)

Abstract: In this study, two possible persistent anomalies of the Madden-Julian Oscillation mode (MJO) are found in the summer season (persistently Pacific active and Indian Ocean active), and an index is set to define the intensity of the two modes. They are proved to have high statistical correlations to the later ENSO events in the autumn and winter seasons: When persistent anomaly of MJO happens in the Pacific Ocean in summer, El Niño events are often induced during the autumn and winter seasons of that year. However, during the other MJO mode when the summer persistent anomaly of MJO occurs in the Indian Ocean, La Niña events often follow instead. The analysis of the atmospheric circulation field indicates that persistent anomaly of MJO can probably affect the entire Equatorial Pacific circulation, and results in wind stress anomalies. The wind stress anomalies could excite warm or cold water masses which propagate eastwards at the subsurface ocean. The accumulation of warm or cold subsurface water in the Equatorial Eastern Pacific Ocean may eventually lead to the formation of an ENSO.

Key words: MJO; ENSO; wind stress; sea surface temperature anomaly; subsurface ocean temperature anomaly
CLC number: P732 **Document code:** A
doi: 10.16555/j.1006-8775.2016.S1.003

1 INTRODUCTION

In the early 1970s, Madden and Julian determined that 40 to 60-day oscillation exists in the tropical atmospheric wind and pressure fields. It is now referred to as MJO (Madden-Julian Oscillation), the most dominant physical mode of tropical intraseasonal variability (Madden and Julian[1, 2]). Following the Empirical Orthogonal Function (EOF) analysis of the three physical variables (OLR, U200 and U850), it was determined by Wheeler and Hendon that two very significant activity centers of the MJO exist in the Indian Ocean (EOF1) and the western Pacific Ocean (EOF2)[3]. On this basis, real-time multivariate MJO index (RMM), the most commonly used MJO index, was defined. Subsequently, the 200 hPa velocity potential data were used for EEOF analysis by Xue[4]. This was followed by projecting these data onto 10 spatial fields of the first EEOF model. After the final step of normalizing, a new MJO index was established. This index is widely used for climate predictions by the U.S. NOAA Center for Weather and Climate Prediction. Although MJO's structure and propagation characteristics are relatively well understood (Madden[5]; Murakami et al. [6]; Krishnamurti and Subrahmanyam[7]; Yasunarl[8]), physical mechanisms involved in interannual and longer-term variations are much less clear (Hendon et al.[9]; Slingo et al.[10]; Waliser and Lau[11]).

ENSO, the interrelated tropical Pacific El Niño and Southern Oscillation (SO), was determined by Bjerknes in 1966 [12]. After that series of analysis and discussions have been carried out regarding the occurrence mechanism and influence range of such large-scale ocean-atmosphere interactions (Li[13]; Jin[14]; Zhang[15]; Cane et al.[16]; Wyrtki[17]; Cao[18]; Chen et al.[19]). Research results have shown that initial sea surface temperature anomaly (SSTA) occurs in a warm pool. Then, the positive temperature anomaly (the 20°C isotherm in particular), along with a west wind anomaly, continuously spreads to the east, with its intensity enhanced by the process of propagation. It continues to spread east and deepen in intensity (Zhang[20]). Further research showed that the subsurface ocean temperature anomaly (SOTA) of Western Pacific warm pool was the source of the ENSO (Zhang and Chao[21]; Mu and Li[22]; Li et al.[23]; Liu et al.[24]). While undergoing the agitation of the Equatorial Western Pacific abnormal zonal winds, the sub-surface warm water mass spreads from the

Received 2015-11-13; **Revised** 2016-03-15; **Accepted** 2016-07-15
Foundation item: National Natural Science Foundation of China (41375059); National Public Welfare (Meteorological Sector) Special Project of China (GYHY201306022)
Biography: YAN Xin, Ph.D. candidate, primarily undertaking research on air-sea interaction and climate change.
Corresponding author: JU Jian-hua, e-mail: jujh@cma.gov.cn

Western Pacific warm pool towards the east (Huang[25]). ENSO, as the strongest interannual signal in the climate system, not only directly causes changes in the tropical Pacific Ocean weather climate system, but also makes significant indirect impacts on the weather and climate of the extra-Equatorial Pacific, along with many other parts of the world, in a variety of ways.

The MJO and ENSO are two types of meteorological phenomena which are quite different in temporal and spatial scale. A series of scientific discussions have been carried out regarding the relationship between the two. In the research conducted by Lau[26], it was determined that the MJO could induce El Niño events by way of atmospheric coupling. Consistent evidence has shown that the Equatorial Mid-western Pacific MJO generally becomes intensified before El Nino, whereas shows a weakening trend during the period of an El Niño, with its vertical structure tending to be barotropic (Lau[27]; Zhang and Gottschalck[28]; Li and Long[29]; Zhai et al.[30]; Kessler and Kleeman[31]; Li and Liao[32]; Li and Li[33]; Li and Zhou[34]). Research shows that the strength of Boreal Summer Intraseasonal Oscillation （BSISO）has obvious correlation with ENSO development and decline (Lin and Li[35]). Therefore, based on the MJO index defined by the global wind field and convection, Slingo et al. pointed out that the MJO might not be the essential factor for the formation of El Niño, but could be a key factor in deciding its growth rate and amplitude[10]. Roundy and Kiladis also showed that during some special events, the MJO contributed to the rapid onset of El Niño while other MJO events were not necessarily associated with such dramatic changes in the equatorial oceanic circulation[36]. Seiki et al. further conclude that although MJO is involved in ENSO development, its efficiency remains largely dependent on the ocean and atmosphere background circulation[37]. Although there are proofs about MJO's positive contribution to El Niño events (Waliser and Lau[11]; McPhaden[20]; Huang et al.[25]; Zhang and Gottschalck[28]; Kessler et al.[38]; Weickmann[39]), but their relationship is still unclear.

As large-scale circulation background field, ENSO have an important effect on global weather and climate change, including MJO. In the study of the interaction between the MJO and ENSO, former studies had been focusing on the relationship between the MJO and El Niño events, with very few of them highlighting the correlation between the MJO and La Niña events . Moreover, at present the influences of the MJO on the formation of the ENSO are not very clear. On the basis of the above researches, a persistent anomaly index used to describe seasonal MJO activities in summer (June to August) in the Indian or Pacific Ocean, is defined in this study. It was found that persistent anomaly of MJO is closely related to the occurrences of the autumn and winter ENSO events, which can be used as an early warning signal of the ENSO events. Finally, the influences of the MJO on the occurrence mechanisms of the ENSO events are also discussed in this study.

2 DATA

(1) The NCEP-DOE re-analysis 2 data were provided by the U.S. National Centers for Environmental Prediction (NCEP) (Kanamitsu et al.[40]). The daily wind field data with the isobaric coordinates (u, v), and the daily sea-level 10 m wind field (u, v) data with the Sigma coordinates, were used with a horizontal resolution of 2.5 ° x 2.5 °.

(2) The daily outgoing longwave radiation data (OLR) were provided by the NCEP, with a horizontal resolution of 2.5°x 2.5 °(Liebmann[41]).

(3) The ten MJO indices were defined by the U.S. National Oceanic and Atmospheric Administration (NOAA), and abbreviated as the Climate Prediction Center (CPC) (Xue et al.[4]). The extended empirical orthogonal function (EEOF) analysis was carried out for these indices by using the 200 hPa velocity potential data. The 10 spatial/temporal fields in the first model were based to define 10 MJO active indices (I_{MJO1}, I_{MJO2}... I_{MJO9}, I_{MJO10}), and each index corresponded to the 10 convective activity centers (80°E, 100°E, 120°E, 140°E, 160°E, 120°W, 40°W, 10°W, 20°E and 70°E), respectively. Therefore, the 10 MJO indices represented the active and inactive status of the MJO activity in the different tropical regions of the Indian Ocean, the Maritime Continent, and the Pacific and Atlantic Oceans. The timeframe of the above data (1), (2) and (3) is from January, 1979 to December, 2012.

(4) The OI SST V2 data with a high resolution of the subsurface ocean temperature were provided by NOAA, of which the spatial resolution was 0.25°×0.25°, and the timeframe was from January, 1981 to December, 2012 (Reynolds et al.[42]).

(5) The Global Ocean Data Assimilation System (GODAS) data were provided by NOAA/OAR/ESRL PSD, with a spatial resolution of 0.33°× 1.0°, depths of 5 to 303 meters and timeframe of January, 1980 to December, 2012. The 26 sub-surface layers are as following: 5 m, 15 m, 25 m, 35 m, 45 m, 55 m, 65 m, 75 m, 85 m, 95 m, 105 m, 115 m, 125 m, 135 m, 145 m, 155 m, 165 m, 175 m, 185 m, 195 m, 205 m, 215 m, 225 m, 238 m, 262 m and 303 m (Behringer and Xue[43]; Behringer et al.[44]; Ji et al.[45]). Detailed information can be obtained from the following website: http://www.esrl.noaa.gov/psd/.

(6) The Oceanic Niño Index (ONI) indices were provided by CPC using a 3-month running mean of ERSST. b3b SST anomalies within the El Niño 3.4

region (5°N - 5°S, 120° - 170°W) (Smith et al.[46]; Xue et al[47]). The timeframe was from January, 1981 to December, 2012.

3 DEFINITION OF PERSISTENT ANOMALY OF MJO INDEX

Under normal circumstances, the MJO active center propagates eastward around the Equator. But in the monitoring of the MJO, it was found that during the summer seasons, the MJO frequently presents insignificant eastward propagation. Insignificant eastward propagation has two typical persistently anomaly forms: one is that MJO persistent anomaly activity stay in the Pacific Ocean with insignificant eastward propagation (in the summer of 1997), the other is that MJO persistent anomaly activity stay in the Indian Ocean with insignificant eastward propagation (in the summer of 1998). The direct impact of such persistent anomaly of MJO activities is to cause tropical convections to continued focus on the Pacific and Indian Oceans, and thus led to anomalies of the tropical atmospheric circulation.

This abnormal situation has significantly displayed on the MJO index of CPC and RMM. After a comparative analysis of the two indices, we found that the MJO index of the CPC can reflect more the character of MJO persistently anomaly. Therefore, the MJO index of the CPC can potentially be used to further define the persistent anomaly index I_{ip} describing the summer seasonal (June - August) MJO activities, as illustrated in Equation (1).

$$I_{ip} = \frac{1}{3}\sum_{i=6}^{8}\left[\left(I_{MJO10} + I_{MJO1}\right) - \left(I_{MJO5} + I_{MJO6}\right)\right]_i \quad (1)$$

Among the 10 MJO indices of the CPC, the I_{MJO10} (70°E) and I_{MJO1} (80°E) can represent the MJO activity degree in the Indian Ocean, and the I_{MJO5} (160°E) and I_{MJO6} (120°W) can represent MJO activity degree in the Pacific Ocean. Equation (1) calculate the difference of the MJO activity degree between in the Indian Ocean and in the Pacific Ocean, then compute average from June to August. It is used to express the character of MJO persistently anomaly. Therefore, it can be concluded that when the I_{ip} is negative, the greater its value is, the higher the MJO activity degree in the Indian Ocean will be; When it is positive, it generally has positive correlations with the MJO activity degree in the Pacific Ocean; and when it is close to 0, the MJO activity would more likely be normal during that year, with west-to-east propagation being normal and no stagnation occurring, and it is also might be the case of the MJO to be basically inactive throughout the world.

After calculating the decadal time series of I_{ip} index, the previous eight years greater than 1 were selected for the high-value typical years (June - August MJO activities in the Pacific Ocean during the years including 1982, 1986, 1987, 1990, 1991, 1997, 2002, and 2009), and the previous eight years less than -1 were selected for the low-value typical years (June - August MJO activity in the Indian Ocean during the years including 1988, 1995, 1996, 1998, 1999, 2007, 2008, and 2010) . They were selected for the composite analysis.

In the composite analysis diagram of the MJO in the typical years of the I_{ip} index (Fig. 1), the distribution characteristics of the persistent anomaly of the MJO defined in this study can be clearly seen. Two special cases existed in the summer seasonal MJO activity in the Pacific and Indian Oceans. In the high-value years of the I_{ip} index (Fig. 1a), beginning in May, the MJO activity at 70 ° E - 80 ° E in the Equatorial Indian Ocean was persistently weakening, and correspondingly the MJO activity at 160 ° E - 120 ° W of the Equatorial Western Pacific was persistently intensifying. The anomaly occurred in the eastward propagation of the MJO, manifesting as the MJO active center becoming stagnated in the Equatorial Mid-Pacific. This process continued until September. Then the MJO active center moved from the Mid-Pacific Ocean eastward towards the Eastern Pacific Ocean, and became stagnated by October. In contrast, in the low-value years of the I_{ip} index (Fig. 1b), the MJO activity in the Indian Ocean enhanced persistently from June to October, with its active center consistently stagnated and maintained in the Indian Ocean, while that in the Pacific Ocean continuously weaken.

During the abnormal stagnation of the MJO active center, the MJO signals in the two oceans vary in intensity. However, either in the Indian or Pacific Oceans, periodic oscillation still existed. For the MJO with persistent anomalies, the active center of the fluctuations only appeared in the Indian Ocean or the Pacific Ocean, while the low phase existed in the other oceans. The states were exactly the opposite. That is to say, the active center of the MJO was stagnated in the Indian and Pacific Oceans, with insignificant eastward propagation. It can be concluded from the above analysis that the defined I_{ip} index was indicative of the persistent abnormal characteristics of the MJO active center in the Pacific and Indian Oceans.

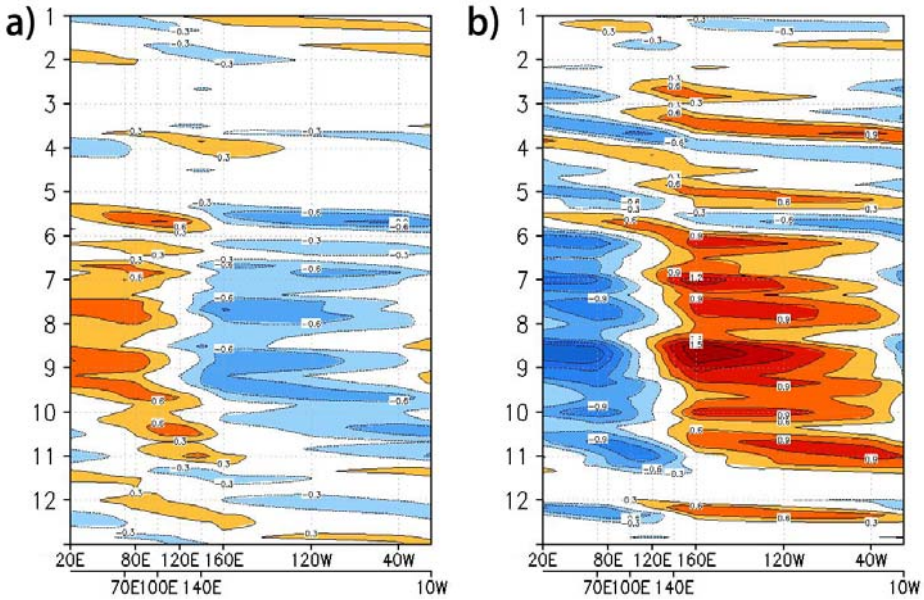

Figure 1. Composite diagram of MJO index of CPC in the typical high-value years (a), and low-value years (b), of I_{ip} index using the longitudinal as abscissa and the months as the *y*-coordinate.

4 COMPOSITE ANALYSIS ON THE INFLUENCE OF PERSISTENT ANOMALIES OF MJO ON THE PACIFIC SST

4.1 *Correlation between the persistent anomalies of MJO and ENSO*

The correlation coefficient between the summer I_{ip} index, the winter SSTA of each year was calculated, and the results are shown in Fig. 2. As viewed from the correlation between the I_{ip} index and the winter SST, as shown in Fig. 2, the intensity of the persistent anomalies of MJO from June to August has a very significant correlation to the winter SST. A positive correlation existed in the Equatorial Mid-Eastern Pacific, where the highest positive-correlation area was located in the central equatorial Pacific Ocean, which reached above 0.8. However, a negative correlation area existed from the Equatorial Western Pacific to the mid-high latitudes, where the highest negative correlation was located in the east sea areas of Australia and the Philippines, and exceeded 0.6. A positive correlation occurred in the Indian Ocean. This positive correlation was located in the mid-western Equatorial Indian Ocean, extending from the Arabian Sea the south of Indian Peninsula, and then southwards to South Indian Ocean. Therefore, the entire SST correlation area showed a positive-negative-positive distribution, which was consistent with the typical SST distribution mode of an ENSO.

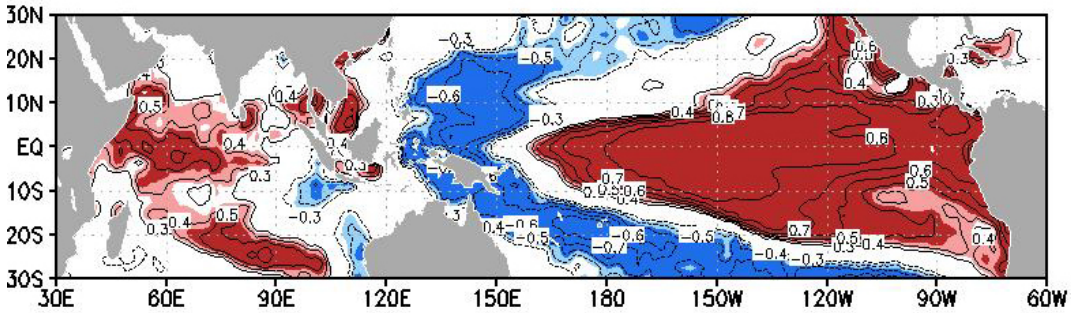

Figure 2. Distribution diagram of correlation coefficient between summer I_{ip} index and winter SST. The shadowed areas indicate the 0.05 and 0.01 significance levels, respectively.

The Niño 3.4 area of SST is an international criterion used to measure the occurrence of ENSO events (Li and Zhao[48]). In Fig. 2 it can be seen that the highest correlation area was located in the Niño 3.4 area. Therefore, the calculated 1980 to 2012 winter ONI index was associated with the summer I_{ip} index. As shown in Fig. 3, the time series of the I_{ip} index had a very good corresponding relationship with the ONI index, and the correlation coefficient was 0.87. This also illustrates that the persistent anomalies of MJO have a very high correlation with the winter SST. Therefore, during the I_{ip} high-value

years, the summer seasonal MJO shows persistent abnormal activity in the Pacific Ocean, which corresponds to the occurrence of El Niño events in the Pacific Ocean. However, during the I_{ip} low-value years, the summer seasonal MJO shows persistent abnormal activity in the Indian Ocean, which corresponds to the occurrence of La Niña events in the Pacific Ocean.

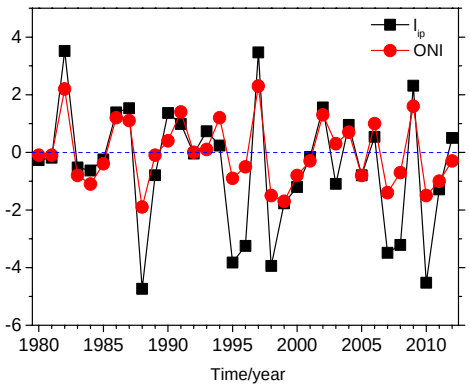

Figure 3. Observed decadal time series of the summer I_{ip} index (the black square), and the winter ONI index (the red circle) for the period 1979-2012.

Further, we make the composite diagram of the winter SST anomaly during the typical years of the I_{ip} index. In the high-value typical years (Fig. 4a), the area with the most significant positive SST anomalies appeared in the mid-eastern Pacific Ocean. The anomaly intensity center was located in the equatorial 170° W - 110° W, where the warm tongue stretched from the coast of Peru to the vicinity of the date line. The SST in the Northwest Pacific and South Pacific Oceans showed negative anomalies, although the SST in the Indian Ocean showed a positive anomaly, and the high-value area was located in the middle of the South Indian Ocean. However, in the low-value typical years (Fig. 4b), significant negative anomalies in the SST existed in the Mid-Eastern Pacific Ocean, of which the center appeared to be more elongated when compared with the high-value years, and extended westward to the date line, before also arriving at 120 ° E in the east. A positive anomaly existed in the Northwest and South Pacific Ocean, and a weak and insignificant negative anomaly occurred in the Indian Ocean. However, a small piece of positive anomaly did appear in the eastern waters near Australia. The typical ENSO modes can be seen in the composite analysis diagrams of the winter SST anomaly in the typical high-value and low-value years of the I_{ip} index.

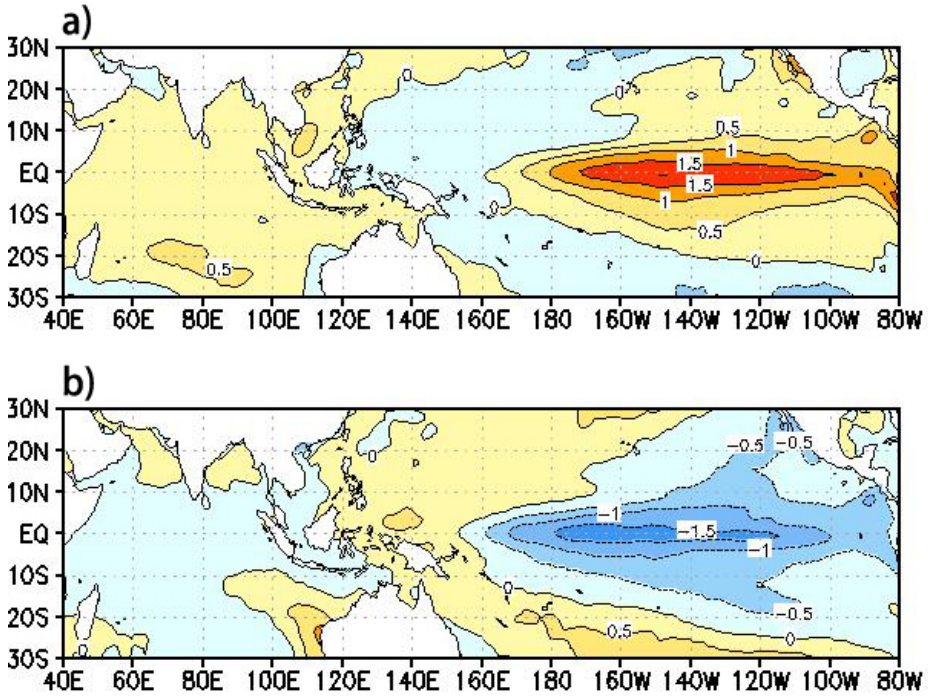

Figure 4. The composite distribution of the winter SSTA corresponding to the typical years of the I_{ip} index (unit:℃); (a) winter SSTA in the high-value years of the I_{ip} index; and (b) winter SSTA in the low-value years of the I_{ip} index.

Thus, significant correlation between the Persistent Anomaly of MJO in summer and Eastern Pacific SST in fall and winter could be determined. Based on it, the persistent anomaly of MJO in summer is a forecast signal for ENSO. These results provide early forecasted basis for relative short-range climate prediction.

4.2 *ENSO occurrence process in the typical years of*

persistent anomaly of MJO

It can be concluded from the previous section that the summer persistent anomaly of MJO were closely related to the autumn and winter Pacific Ocean temperature.

ENSO is formed by the subsurface ocean temperature anomaly (SOTA) propagating from the Western Pacific Ocean to the Eastern Pacific Ocean (Li and Mu[49]). Mcphaden's studies have pointed out that the SST anomaly of the ENSO appears initially in the warm pool[20]. It can be found through further analysis that the SOTA of the Western Pacific warm pool was the source of the ENSO occurrence. Another research shows that, there is a "see-saw"phenomenon between the subsurface (120～160m) temperature anomaly in Western Pacific and the subsurface (40～60m) temperature anomaly in Eastern Pacific what is out of phase to each other (Mu and Li[22]). After the subsurface temperature anomaly appearing in Western Pacific, this anomalous signal transfers east along equatorial thermocline, and expanded continuously to surface Eastern Pacific. Therefore, the changes to the subsurface ocean temperature anomaly in the Eastern Pacific Ocean could serve as indications of ENSO development.

The composite Equatorial Pacific 5 to 300 m monthly SOTA diagram for the high-value years of the I_{ip} index was used to investigate the formation process of the El Niño events which were correlated to the persistent Pacific anomalies of MJO, and the results are shown in Fig. 5. The El Niño events were generated in July (Fig. 5a), when a weak warm water mass was gradually formed in the mid-eastern Pacific, while very weak cold water existed in the west, thereby displaying a status of cold in the west, and warm in the east. A significant change occurred in August (Fig. 5b), when the temperature anomaly of subsurface warm water mass's center reached above 2.5℃, with a gradual eastward extension along the thermocline in the eastern section of the mid-eastern Pacific Ocean, at 150°W during the autumn season. The cold water mass had rapidly increased in the western warm pool, where the central temperature anomaly reached more than 1°C, and slowly developed to the vicinity of the date line. In September (Fig. 5c), the warm water mass center was located in the eastern Pacific Ocean at 160°W - 120°W, with a depth of 60 to 150 m. The cold water mass's center had reached beyond 150° E, and was approaching the date line. The temperature gradient between the cold and warm water masses increased as the temperature difference intensified. In October (Fig. 5d), warm water mass's center had continued to intensify near 120° W, and the cold water mass's center was intensified at 120° E - 150° E, which led to further increases in the temperature differences. During November and December (Figs. 5e, f), the confrontation between the cold and warm water masses occurred in the eastern and western Pacific Ocean, when the maximum temperature difference reached more than 6℃. The intensifying and eastward movement of cold water mass squeezed the warm water mass towards the eastern coast. This was an El Niño event.

In the low-value years of the I_{ip} index, the MJO was persistently active in the Indian Ocean, while inactive in the Pacific Ocean. In the composite Equatorial Pacific 5 to 300 m monthly SOTA diagram during the low-value years of the I_{ip} index (Fig. 6), it can be clearly seen that under the influence of persistently inactive MJO, the subsurface ocean temperature showed a weak status of warm in the west, and cold in the east during July (Fig. 6a). In August (Fig. 6b), a great warming occurred to the centers of the warm water masses, anomaly center appeared near 130°E. From September to October (Fig. 6c, d), a negative anomaly center of western Pacific Ocean warm water mass was intensified eastward. At the same time, a positive anomaly center of cold water mass in the mid-eastern Pacific Ocean rapidly and continuously developed, with an eastward extension along the thermocline. A confrontation between the cold and warm water mass existed near the date line. In November and December (Figs. 6e, f), the temperature gradient of the cold and warm water masses continuously deepening. The warm water mass was eastward beyond the date line, and squeezed toward the cold water mass, forcing a surface lift of the cold water mass. This was a La Niña event.

It can be concluded from the above composite analysis that, excited by the influence of persistent anomalies of MJO in summer, the temperature differences of the cold and warm subsurface ocean temperature in the Eastern and Western Pacific Ocean increase in, as well as the Eastern Pacific's SOTA expanded towards the sea surface along the thermocline. As a result, the occurrence of ENSO event was induced.

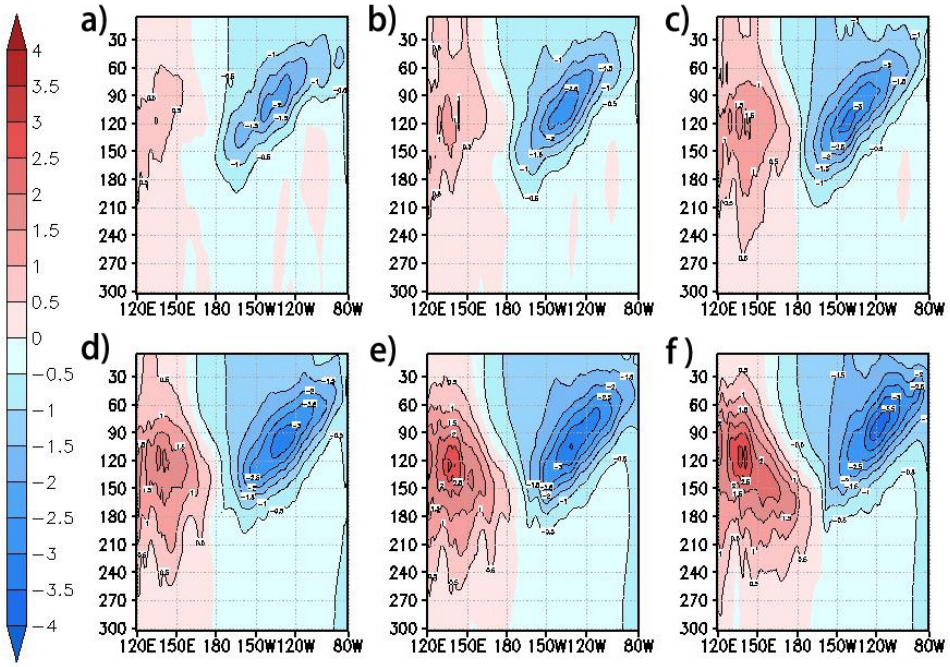

Figure 5. The composite monthly SOTA during the high-value typical years of the I_{ip} index (unit:℃), using the longitudinal as abscissa and the ocean depth (0-300m) as the *y*-coordinate; (a), (b), (c), (d), (e), and (f) are the anomaly composites from July to December, respectively.

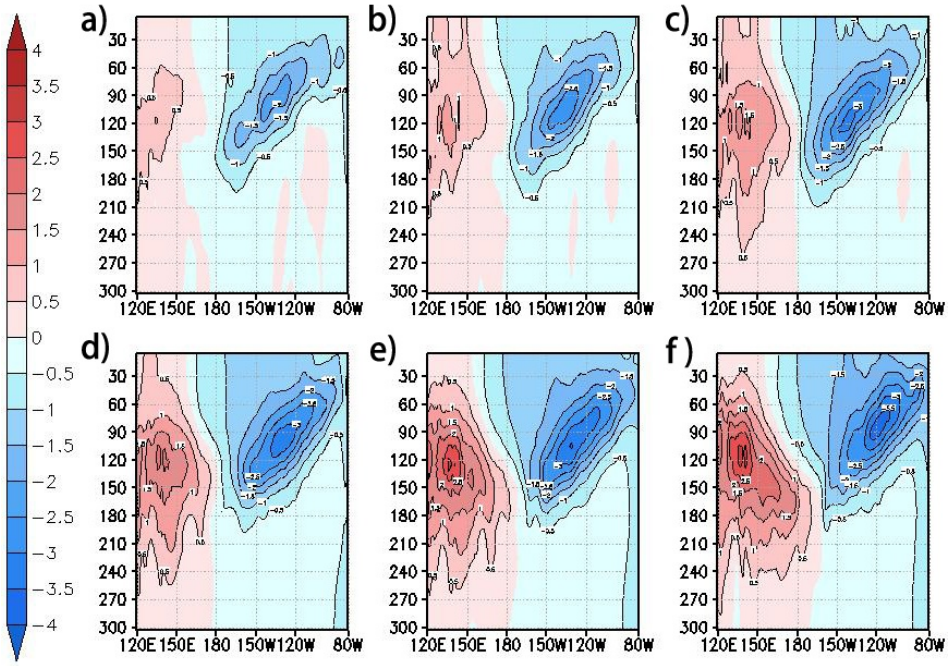

Figure 6. The composite monthly SOTA during the low-value typical years of the I_{ip} index (unit: ℃), using the longitudinal as abscissa and the ocean depth (0-300m) as the *y*-coordinate; (a), (b), (c), (d), (e), and (f) are the anomaly composites from July to December, respectively.

4.3 *Analysis of circulation field of persistently abnormal MJO and its influence on the occurrence process of ENSO*

The analysis of the changes of the atmospheric circulation undergoing persistent anomalies of MJO, and the resulting changes to the sea surface wind stress has been presented. Through the analysis of the changes in the surface sea temperature and subsurface ocean temperature, the intrinsic mechanism that induced action of the persistent anomalies of MJO on the ENSO has been investigated.

First of all, in terms of the circulation field in a climate state, a Walker Circulation exists over the Pacific Ocean. Due to the nature of the Pacific Ocean (warm in the west and cold in the east), warm moist air rises in the west with high-level westerly winds,

and then sinks in the Eastern Pacific with low-level the eastwardly winds. The Equatorial trade winds blow from the Eastern to Western Pacific Ocean, which leads to the formation of a complete Walker Circulation (Wu and Meng[50]). As viewed from the composite diagram of an anomaly in the high-value years of the I_{ip} index (Fig. 7), 200 hPa over the Pacific Ocean in June showed a significant eastwardly wind anomaly (Fig. 7b), and the low-level 850 hPa showed a westward wind anomaly (Fig. 7c). This is referred to as an anti-Walker Circulation, where the ascending branch was located in the mid-eastern Pacific Ocean. Meanwhile, the OLR active region was also situated east of date line (Fig. 7a), which is consistent with the persistently active of MJO in the Pacific Ocean. This anomaly situation undermined the low-level eastwardly wind of the Walker Circulation, and was more conducive to the development of the warm seawaters in the eastern Pacific Ocean. This anomaly circulation type continued until the end of September. At 60° E - 120° E, the anomalies were shown in the high-level westerly winds and the low-level eastwardly winds. These anomalies were formed due to the abnormal zonal circulation in the Indian Ocean driven by the reverse gear coupling of the Pacific Walker Circulation, where the sinking branch was located in the eastern Indian Ocean. In contrast in the low-value years, beginning in June, high-level westerly winds (Fig. 8b), and low-level eastwardly winds (Fig. 8c) appeared over the Pacific Ocean. This circulation was an intensified Walker Circulation. High OLR values in the Western Pacific represent suppressed convection ,while low OLR values located in the Maritime Continent near 120° E represent increased convection(Fig. 8a). Then beginning September, an eastward wind anomaly appeared at 200 hPa over Maritime Continent (Fig. 8b), and correspondingly, a westerly wind anomaly existed at 850 hPa (Fig. 8c). This zonal circulation in the Indian Ocean driven by the Pacific Walker Circulation was found to be thriving in the autumn and winter seasons. In regards to the OLR field (Fig. 8a), a significant OLR inactive region occurred at 60° E in the western Indian Ocean during September, November and December.

Here we discuss the sequence of the events. (1) The phenomenon of persistent anomaly of MJO occurred mainly in summer, with the strongest signals in August. After that, the phenomenon decreases to be insignificant in winter. (2) OLR and zonal circulation anomaly in the Western Pacific began to appear in summer, then constantly increases. The zonal circulation anomaly would be most prominent during autumn. (3) In most cases, both SST and SOT anomalies appear in autumn. And the most significant sea temperature is in winter. On the above three bases, we consider that only in the beginning of ENSO, it is induced by the persistent anomaly of MJO through the effects of air-sea interaction.

During the analysis of the persistent anomalies of MJO, it was found that the prevailing zonal winds anomalies induced by the Pacific Ocean MJO in the high-value and low-value years of the I_{ip} index were basically the opposite. As a result, the near-sea surface wind stress also showed anomalies. The equation of the 10 m surface wind field used in this study is as follows

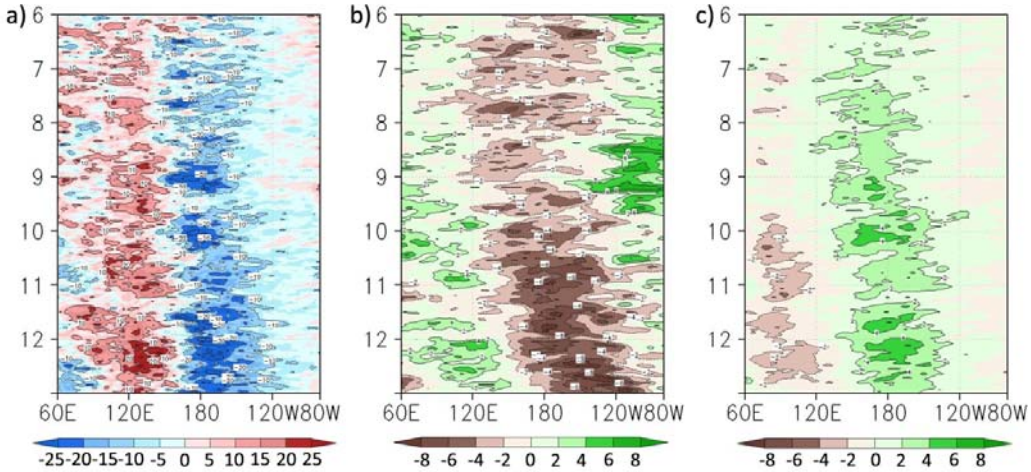

Figure 7. Composite temporal-longitude section of the anomalies in: (a) OLR (Wm^{-2}); (b) U200 (ms^{-1}); and (c) U850 (ms^{-1}) during the high-value typical years of the I_{ip} index. The timeframe was from June to December as the *y*-coordinate, and the location was the equatorial 60°E - 80°W as the abscissa. All these data are equatorially averaged.

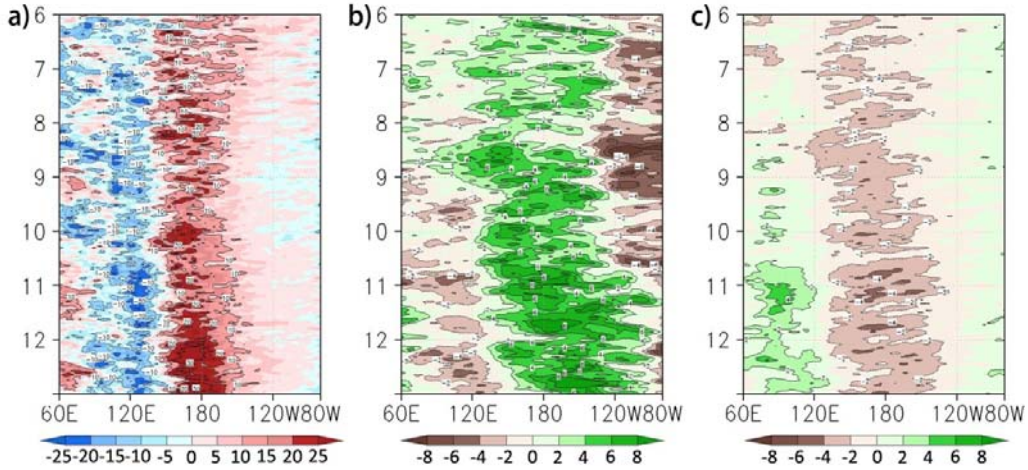

Figure 8. Composite temporal-longitude section of the anomalies in: (a) OLR (Wm^{-2}); (b) U200 (ms^{-1}); and (c) U850 (ms^{-1}) during the low-value typical years of the I_{ip} index. The timeframe was from June to December as the *y*-coordinate, and the location was the equatorial 60°E - 80°W as the abscissa. All these data are equatorially averaged.

$$\tau_x = u\sqrt{u^2 + v^2} \quad (2)$$

The equatorial zonal wind stress was approximately calculated, and the five-day moving average was carried out in order to filter the high-frequency fluctuations (Zhang and Gottschalck[28]). Playing an important role in air-sea interaction, wind stress reflects the drag force of atmosphere on Ocean. Li's research has found that the Equatorial Western Pacific west wind anomaly have a direct relationship with the subsurface ocean temperature anomalies in the warm pool[49]. The anomalies of equatorial westerly and its eastward expanding would be a major reason of eastward subsurface ocean temperature anomalies. Chan tends to emphasize that the positive anomalies of Western Pacific subsurface ocean temperature spread eastwards, only when the strong anomalies of equatorial westerly lasts for 3 or more months over the Middle Pacific(160 °E--160 °W)[51]. Previous studies have shown that after the zonal wind stress displays a positive anomaly, a significant rising occurs in the SST (Huang and Zhang[52]). The fundamental source for ENSO is eastward propagating of the subsurface warm water from the Western Pacific Ocean's warm pool (Zhang and Chao[21]; Li et al.[23]; Chao[53]). It is pointed out that ENSO essentially is an interannual cycle of the tropical Pacific SOTA driving by the anomalies of equatorial westerly (Li[54]).

It can be seen in Fig. 1a that, in the high-value years of the Iip index, the signs of the persistently active of MJO in the Pacific Ocean were evident since May, and the persistent active period was prominently from June to September. Meanwhile, the MJO in Indian Ocean had continued in a weaker state. In the zonal wind stress anomaly diagram corresponding to the high-value years of the Iip index (Fig. 9a), the positive anomaly in weak wind stress continued to appear over the Western Pacific Ocean during June, and the stronger wind stress appeared near the date line beginning in July. With eastward propagating of marine Kelvin wave induced by the Western Pacific Ocean surface wind stress, warm or cold water propagated from the Western Pacific Ocean to the east, the study found (Zhang and Gottschalck[28]). The eastward drag force was generated to the wind stress, then induced the eastward propagation of marine Kelvin wave. The warm marine Kelvin wave could bring the subsurface warm water from the Western Pacific Ocean to the east (Zhang and Chao[21]; Chen and Wang[51]; Huang and Zhang[52]; Chao[53]). In the eastern Pacific Ocean, accumulation of subsurface warm water might result in the increased eastern Pacific Ocean SST and SOT.

In the Composite temporal-longitude section of SOTA (Fig.9), the 0.5℃ range of the Eastern Pacific SOTA (Fig. 9b) had significantly expanded in August. From the end of September to the beginning of October, there was a positive anomaly which was significantly higher than 1℃. Correspondingly, a 0.5 ℃ negative anomaly occurred in the western Pacific at the beginning of August, and then continued to expand. A 1℃ negative anomaly appeared until early October. The Eastern and Western Pacific Oceans' subsurface ocean temperatures experienced an apparent reverse change relationship. The trend of cold in the west and warm in the east was intensified rapidly over time. Moreover, in the Composite temporal-longitude section of SSTA (Fig. 9c), the 1℃ positive anomaly in the Eastern Pacific SSTA appeared successively in August, and became stable in September and October, with an intensifying trend.

The Western Pacific SSTA showed a weak negative anomaly. Finally in November and December, both the SST and SOT were fully developed. When the Eastern SSTA showed a positive anomaly above 1.5 ℃. This led to the formation of an El Niño event.

In contrast, in the low-value years of the I_{ip} index, the areas with persistently active of MJO were located in the Indian Ocean beginning in June, while the Pacific MJO was abnormally weak (Fig. 1b). This situation was particularly significant in August and September, and continued until early November. As viewed from the zonal wind stress anomaly field (Fig. 10a), the persistent negative anomaly could be seen beginning in July, while the stronger negative anomaly appeared after October, when the negative anomaly of the entire Western Pacific zonal wind stress was abnormally prosperous in autumn and winter. A westward drag force was generated by the wind stress, which induced the eastward propagation of cool marine Kelvin wave. This cool marine Kelvin wave led to the eastward propagation of the subsurface cold water from the Western Pacific Ocean to the east. As well as accumulation of subsurface warm water in the Eastern Pacific Ocean, SST and SOT might be reduce (Zhang and Chao[21]; Chen and Wang[51]; Huang and Zhang[52]; Chao[53]) . Beginning in July, the negative SOTA below 0.5 ℃ appeared in the Western Pacific Ocean (Fig. 10b), and in August, a positive value above 0.5 ℃ occurred in the Eastern Pacific Ocean. In the type of situation up until September, a negative value greater than 1 ℃ appeared in the Western Pacific Ocean, and the Western Pacific positive value center occurred in the anomaly greater than 1℃ at the end of October. The situation of warm in the west and cold in the east developed to a peak in November and December. As viewed from the performance of the SSTA (Fig. 10c), the cold seawater with a stable negative anomaly of 1 ℃ appeared in the western region of the Eastern Pacific Ocean at 120° W near the end of September, which continued with an extension development eastwards throughout the entire Eastern Pacific Ocean in December. When both the SST and SOT showed a negative anomaly in November and December, it would led to the formation of a La Niña event.

From another angle, the influence of wind stress on ocean current might be one of the causes of ENSO. During the high-value years of the I_{ip} index, the easterly wind stress dragged the Equatorial Pacific surface currents to the east, which led toward the onshore currents in the Equatorial Eastern Pacific Ocean, and therefore the Equatorial warm water appeared in the Eastern Pacific Ocean. Combined with the eastward movement of the subsurface warm water previously mentioned, the warm water gathered in the Eastern Pacific Ocean and accelerated the formation of an El Niño event. In the low-value years of the I_{ip} index, the westerly wind stress dragged the Equatorial Pacific surface currents to the west, which led toward the offshore currents in the Equatorial Eastern Pacific Ocean. Due to the divergence in the surface seawater, the cold water welled upward and accelerated the formation of a La Niña event.

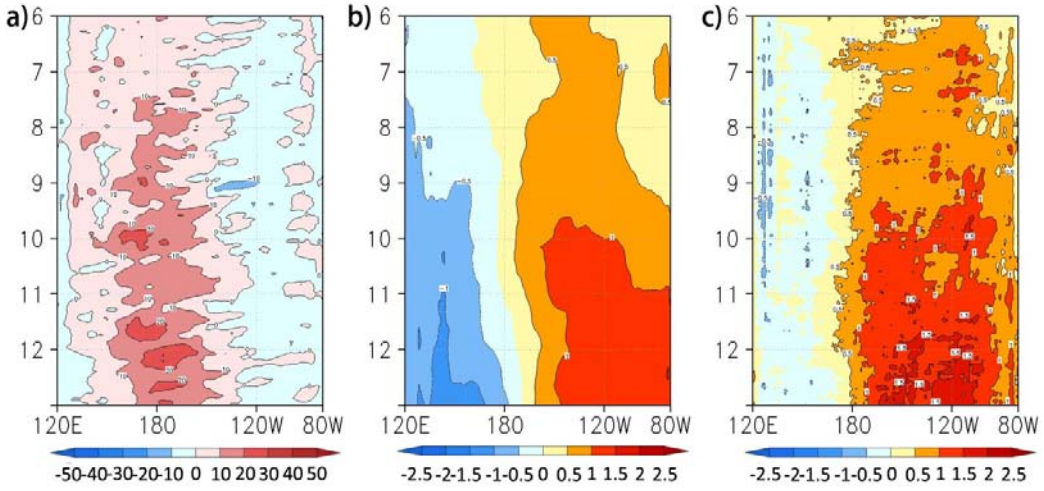

Figure 9. Composite temporal-longitude section of: (a) 5 d moving average wind stress; (b) SOTA; and (c) SSTA in the high-value typical years of the I_{ip} index. The timeframe was from June to December, and the location was the equatorial 60° E - 80° W.

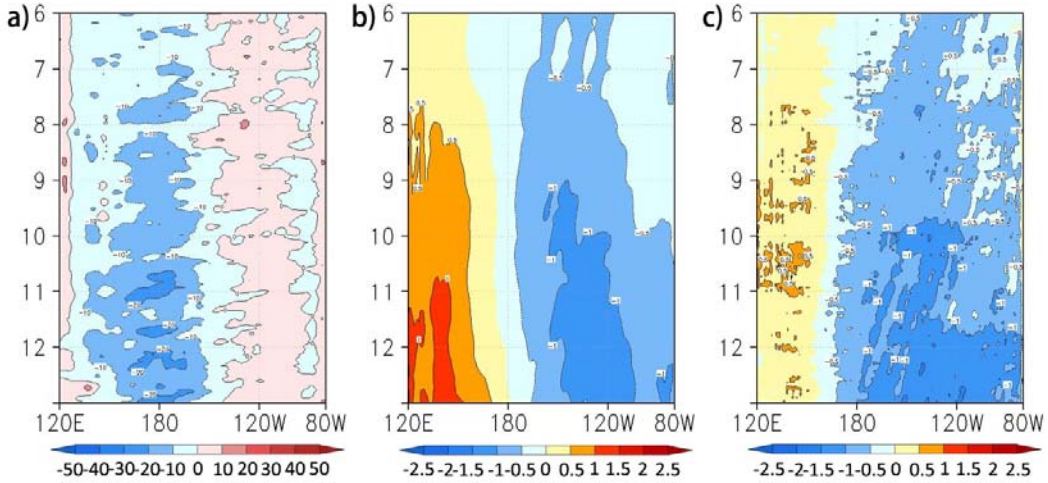

Figure 10. Composite temporal-longitude section of: (a) 5 d moving average wind stress; (b) SOTA; and (c) SSTA in the low-value typical years of the I_{ip} index. The timeframe was from June to December, and the location was the equatorial 60° E - 80° W.

5 CONCLUSIONS AND DISCUSSION

(1) The eastward propagation of the MJO was not regular. In some special cases, it was persistently active in the Indian or Pacific Oceans with eastward propagation being insignificant. The persistent anomalies of MJO were observed, and they were found to be more significant in the summer season. The I_{ip} index was defined in this article to describe the persistent anomaly characteristics of MJO in the Indian and Pacific Oceans.

(2) It was found that the intensity of the persistent anomalies in the summer MJO had a significant correlation to the autumn and winter Equatorial Eastern Pacific ocean temperature. Therefore, the persistent anomalies of MJO could be taken as predictive signals of the ENSO occurrences. If the summer MJO shows persistent abnormal activity in the mid-western Pacific Ocean, then warm waters will be continuously accumulated in the Eastern Pacific Ocean, and thus induce an El Niño event. In contrast, if the summer MJO displays persistently abnormal activity in the Indian Ocean, while the Western Pacific is abnormally inactive, the cold water will be continuously accumulated in the Eastern Pacific, and a La Niña event will happen. These results provide early forecasted basis for relative short-range climate prediction.

(3) The internal mechanism of the MJO affecting the ENSO occurrence was studied. This included the following conclusions: (1) if the summer Western Pacific MJO is persistently abnormally strong, then a persistent positive anomaly could occur to the zonal wind stress, and induce a warm marine Kelvin wave. The warm marine Kelvin wave could bring the subsurface warm water from the Western Pacific Ocean to the east, resulting in corresponding changes in the subsurface and surface temperatures. Then, the Equatorial Western Pacific ocean temperature will show a cooling trend, while the Eastern Pacific ocean temperature shows a warming trend. With accumulation of subsurface warm water in the autumn and winter seasons, there would be an El Niño event forming; (2) if the summer Western Pacific MJO shows weak persistent anomalies, then a persistent negative anomaly will occur to the zonal wind stress, and induce a cold marine Kelvin wave. The cold marine Kelvin wave could bring the subsurface cold water from the Western Pacific Ocean to the east, resulting in corresponding changes in the subsurface and surface temperatures. Then the phenomenon of the Equatorial Western Pacific ocean temperature warming, while the Eastern Pacific ocean temperature cools will occur. With accumulation of subsurface warm water in the autumn and winter seasons, there would be a La Niña event forming.

In this study, a composite analysis was used to discuss the physical mechanisms of the MJO which affect the ENSO. Because of this method, the activities and propagation of the marine Kelvin wave could not be displayed well. Therefore, it is unable to carry out a detailed analysis. In later studies, some special cases will be utilized in order to further explore the intrinsic mechanism of the persistent anomalies of MJO on the ENSO.

REFERENCES:

[1] MADDEN R A, JULIAN P R. Detection of a 40–50 Day Oscillation in the Zonal Wind in the Tropical Pacific[J]. J Atmos Sci. 1971, 28(5): 702-708.

[2] MADDEN R A, JULIAN P R. Description of Global-Scale Circulation Cells in the Tropics with a 40–50 Day Period[J]. J Atmos Sci, 1972, 29(6): 1 109-1 123.

[3] WHEELER M C, HENDON H H.. An all-season real-time multivariate MJO index: Development of an index for monitoring and prediction [J]. Mon Wea Rev [H.W. Wilson - AST], 2004, 132(8): 1 917-1 932.
[4] XUE Y, HIGGINS W, KOUSKY V. Influences of the Madden Julian Oscillations on temperature and precipitation in North America during ENSO-neutral and weak ENSO winters [C]// Proc. Workshop on Prospects for Improved Forecasts of Weather and Short-Term Climate Variability on Subseasonal (2 Week to 2 Month) Time Scales. 2002.
[5] MADDEN R A. Seasonal variations of the 40-50 day oscillation in the tropics [J]. J Atmos Sci, 1986, 43(24): 3 138-3 158.
[6] MURAKAMI T, NAKAZAWA T, HE J. On the 40-50 day oscillations during the 1979 Northern Hemisphere summer. I: Phase propagation [J]. J Meteorol Soc Jpn. 1984, 62(3): 440-468.
[7] KRISHNAMURTI T N, SUBRAHMANYAM D. The 30–50 Day Mode at 850 mb During MONEX [J]. J Atmos Sci, 1982, 39(9): 2 088-2 095.
[8] YASUNARI T. A quasi-stationary appearance of 30 to 40 day period in the cloudiness fluctuations during the summer monsoon over India [J]. Meteorol Soc Jpn. 1980, 58: 225-229.
[9] HENDON H H, ZHANG C D, GLICK J D. Interannual variation of the Madden-Julian oscillation during austral summer[J]. J Climate. 1999, 12(8): 2 538-2 550.
[10] SLINGO J M, ROWELL D P, SPERBER K R, et al. On the predictability of the interannual behaviour of the Madden‐Julian Oscillation and its relationship with El Niño [J]. Quart J Roy Meteorol Soc, 1999, 125(554): 583-609.
[11] WALISER D, LAU W K-M. Intraseasonal Variability in the Atmosphere-Ocean Climate System [M]// Intraseasonal Variability in the Atmosphere-Ocean Climate System, WALISER D, LAU WK-M, 2005 XVIII, 474 p. 80 illus. 3-540-22276-6. Berlin: Springer, 2005.
[12] BJERKNES J. A possible response of the atmospheric Hadley circulation to equatorial anomalies of ocean temperature [J]. Tellus A. 1966, 18(4):
[13] LI Chong-yin. An introduction to the Climate Dynamics [M]. Beijing: China Meteorological Press, 2000.
[14] JIN F F. An equatorial ocean recharge paradigm for ENSO. Part II: A stripped-down coupled model [J]. J Atmos Sci, 1997, 54(7): 830-847.
[15] ZHANG Ren-he. A comprehensive review of the researches on the mechanisms of ENSO cycles and their modelling and prediction [J]. Adv Earth Sci, 1993, 06: 50-56.
[16] CANE M A, ZEBIAK S E, DOLAN S C. Experimental forecasts of El Niño [J]. Nature. 1986, 321(6073): 827-832.
[17] WYRTKI K. El Niño-The dynamic response of the equatorial Pacific ocean to atmospheric forcing [J]. J Phys Oceanogr, 1975, 5: 572-584.
[18] CAO Lu, SUN Cheng-hu, REN Fu-min, et al. Study of a comprehensive monitoring index for two types of ENSO events [J]. J Trop Meteorol, 2015, 21(2): 153-160.
[19] CHEN Yi-de, ZHANG Ren, JIANG Guo-rong. Summary of Chinese research on ENSO in recent years [J]. J Trop Meteorol, 2005, 21(6): 634-641.
[20] MCPHADEN M J. Genesis and evolution of the 1997-98 El Nino [J]. Science. 1999, 283(5404): 950-954.
[21] ZHANG Ren-he, CHAO Ji-ping. Some new aspects in understanding of ENSO cycle [J]. Clim Environ Res, 2002, 7(2): 175-183.
[22] MU Ming-quan, LI Chong-yin. Interaction between Western Pacific warm pool SOTA and ENSO circulation [J]. Chin J Atmos Sci, 2000, 4: 447-460 (in Chinese).
[23] LI C Y, MU M Q, ZHOU G Q. The variation of warm pool in the equatorial western Pacific and its impacts on climate [J]. Adv Atmos Sci, 1999, 16(3): 378-394.
[24] LIU Zheng-qi, LIU Yu-guo, HA Yao, et al. Role of equatorial Pacific Ocean subsurface oceanic temperature mode in ENSO cycle [J]. J Trop Meteorol, 2014, 20(4): 334-341.
[25] HUANG Wei, CAO Jie, HUANG Xiao, et al. The evolution of 20°C isothermal depth in tropical Pacific and its association with ENSO cycle [J]. J Trop Meteorol, 2011, 27(1): 82-88.
[26] LAU K M, CHAN P H. The 40–50 day oscillation and the El Niño/Southern Oscillation: A new perspective [J]. Bull Amer Meteorol Soc, 1986, 67(5): 533-534.
[27] LAU K M. El Niño Southern Oscillation– climate connections [M]// Intraseasonal Variability in the Atmosphere-Ocean Climate System, LAU K M, WALISER D E, New York: Springer, 2005.
[28] ZHANG C, GOTTSCHALCK J. SST anomalies of ENSO and the Madden-Julian oscillation in the equatorial Pacific [J]. J Climate, 2002, 15(17): 2 429-2 445.
[29] LI Chong-yin, LONG Zhen-xia. Intraseasonal oscillation anomalies in the tropical atmosphere and the 1997 EI Nino occurrence [J]. Chinese J Atmos Sci, 2001, 25(5): 589-595.
[30] ZHAI Pan-mao, GUO Yan-jun, LI Xiao-yan. A diagnostics analysis of 1997/1998 ENSO event and the role of intra-seasonal oscillation in the tropical atmosphere [J]. J Trop Meteorol, 2001, 17(1): 1-9.
[31] KESSLER W. S., KLEEMAN R. Rectification of the Madden-Julian oscillation into the ENSO cycle [J]. J Climate, 2000, 13(20): 3 560-3 575.
[32] LI Chong-yin, LIAO Qing-hai. Exciting mechanism of tropical intraseasonal oscillation for El Nino event [J]. J Trop Meteorol, 1998, 14(2): 97-105.
[33] LI Gui-long, LI Chong-yin. Activity of atmospheric intraseasonal oscillation and El Nino [J]. J Trop Meteorol, 1998, 14(1): 55-63.
[34] LI Chong-yin, ZHOU Ya-ping. Relationship between intraseasonal oscillation in the tropioal atmosphere and ENSO [J]. Chin J Geophys. 1994, 37(1): 17-26.
[35] LIN A, LI T. Energy spectrum characteristics of boreal summer intraseasonal oscillations: Climatology and variations during the ENSO developing and decaying phases [J]. J Climate. 2008, 21(23): 6 304-6 320.
[36] ROUNDY P E, KILADIS G N. Observed relationships between oceanic kelvin waves and atmospheric forcing [J]. J Climate. 2006, 19(20): 5 253-5 272.
[37] SEIKI A, TAKAYABU Y N, YONEYAMA K, et al. The oceanic response to the Madden-Julian oscillation and ENSO [J]. SOLA, 2009, 5: 93-96.
[38] KESSLER W S, MCPHADEN M J, WEICKMANN K M. Forcing Of intraseasonal Kelvin waves in the equatorial Pacific [J]. J Geophys Res: Oceans (1978–2012). 1995, 100(C6): 10 613-10 631.
[39] WEICKMANN K M. El Niño/Southern Oscillation and Madden‐Julian (30–60 day) oscillations during 1981–1982 [J]. J Geophys Res: Oceans (1978–2012). 1991, 96(S01): 3 187-3 195.
[40] KANAMITSU M., EBISUZAKI W, WOOLLEN J, et al. NCEP-DOE AMIP-II reanalysis (R-2) [J]. Bull Amer Meteorol Soc, 2002, 83(11): 1 631-1 643.
[41] LIEBMANN B. Description of a complete (interpolated) outgoing longwave radiation dataset [J]. Bull Amer Meteorol Soc, 1996, 77(6): 1275.
[42] REYNOLDS R W, SMITH T M, LIU C, et al. Daily high-resolution-blended analyses for sea surface temperature

[J]. J Climate. 2007, 20(22): 5 473-5 496.
[43] BEHRINGER D W, XUE Y. Evaluation of the global ocean data assimilation system at NCEP: The Pacific Ocean [C]//Preprints, Eighth Symp on Integrated Observing and Assimilation Systems for Atmosphere, Oceans, and Land Surface, Seattle, WA, Amer Meteorol Soc, 2004, 2.
[44] BEHRINGER D W, JI M, LEETMAA A. An improved coupled model for ENSO prediction and implications for ocean initialization. Part I: The ocean data assimilation system [J]. Mon Wea Rev, 1998, 126(4): 1 013-1 021.
[45] JI M., LEETMAA A, DERBER J. An ocean analysis system for seasonal to interannual climate studies [J]. Mon Wea Rev, 1995, 123(2): 460-481.
[46] SMITH T M, REYNOLDS R W, PETERSON T C, et al. Improvements NOAAs historical merged land–ocean temp analysis (1880–2006) [J]. J Climate. 2008, 21(10): 2 283-2 296.
[47] XUE Y, SMITH T M, REYNOLDS R W. Interdecadal changes of 30-yr SST normals during 1871-2000 [J]. J Climate, 2003, 16(10): 1 601-1 612.
[48] LI Xiao-yan, ZHAI Pan-Mao. On indices and indicators of ENSO episodes [J]. Acta Meteorol Sinica, 2000, 58(1): 102-109.
[49] LI Chong-yin, MU Ming-quan. El Nino occurrence and sub-surface ocean temperature anomalies in the Pacific warm pool [J]. Sci Atmos Sinica, 1999, 23(5): 513-521.
[50] WU Guo-xiong, MENG Wen. Gearing between the Indo-monsoon circulation and the Pacific-Walker circulation and the ENSO Part I: Data analyses [J]. Chin J Atmos Sci, 1998, 24(1): 15-25.
[51] CHEN Xing-rong, WANG Zhang-gui. Westerly anomaly, eastward propagation of the subsurface temperature anomaly and El Nino event [J]. Acta Oceanol Sinica, 2003, 25(1): 19-27.
[52] HUANG Rong-hui, ZHANG Ren-he. The dynamics of tropical western pacific zonal wind anomalies on ENSO cycle [J]. Sci China (Ser D), 2001, 31(8): 697-704.
[53] CHAO Ji-ping. ENSO: The harmonic ocean-atmosphere interaction in tropics [J]. Adv Marine Sci. 2002, 20(3): 1-8.
[54] LI Chong-yin. A further study of essence of the ENSO [J]. Clim Environ Res, 2002, 7(2): 160-174.

Citation: YAN Xin, JU Jian-hua and GAN Wei-wei. The influence of persistent anomaly of MJO on ENSO [J]. J Trop Meteorol, 2016, 22(S1): 24-36.